THE BELL SYSTEM TECHNICAL JOURNAL
Vol. 62, No. 9, November 1983
Printed in U.S.A.

Transmission Errors and Forward Error Correction in Embedded Differential Pulse Code Modulation

By D. J. GOODMAN* and C.-E SUNDBERG†

(Manuscript received December 11, 1982)

We have derived formulas for the combined effects of quantization and transmission errors on the performance of embedded Differential Pulse Code Modulation (DPCM), a source code that can be used for variable-bit-rate speech transmission. Our analysis is more general and more precise than previous work on transmission errors in digital communication of analog signals. Special cases include conventional DPCM and Pulse Code Modulation (PCM). Our main result is a signal-to-noise ratio formula in which the effects of source characteristics (input signal, codec design parameters) and the effects of transmission characteristics (modulation, channel, forward error correction) are clearly distinguishable. We also present, in computationally convenient forms, specialized formulas that apply to uncoded transmission through a random-error channel, transmission through a slowly fading channel, and transmission with part or all of the DPCM signal protected by an error-correcting code. Numerical results show how channel coding can have different effects on conventional and embedded DPCM. They also show how the binary-number representation of quantizer outputs influences performance.

I. INTRODUCTION

1.1 Embedded Differential Pulse Code Modulation

Embedded coding can play a valuable role in variable-bit-rate speech transmission. With an embedded code the analog-to-digital (a/d) and

* Bell Laboratories. † University of Lund, Sweden.

digital-to-analog (d/a) converters operate at a constant, high bit rate, and the transmission system controls the instantaneous rate. Proposed applications for variable-bit-rate operation include a digital private branch exchange,[1] digital speech interpolation,[2] packet-switched voice transmission,[3] and mobile radio.[4]

Sophisticated versions of Differential Pulse Code Modulation (DPCM) are promising speech codes for these and other environments.[5–7] However, conventional DPCM is not suited to variable-bit-rate transmission because the decoder amplifies the effects of bit-rate adjustments. On the other hand, a slightly modified form of DPCM avoids this problem and produces an embedded code.[8]

Figure 1 shows the codec (coder, decoder) structure of embedded DPCM. Although up to E bits/sample can be transmitted, the signals presented to the two integrators have a resolution of only M bits/sample, the minimum bit rate of the channel. While Fig. 1 is a useful guide to practical implementations, Fig. 2, which is equivalent, is easier to analyze. It shows the quantizer at the encoder as a successive-approximation combination of two quantizers: a "minimal" quantizer with M bits/sample and a "supplemental" quantizer with E–M bits/sample, operating on the error signal of the minimal quantizer.*

In embedded DPCM, all of the bits from the minimal quantizer arrive at the decoder; the transmission system can delete some or all of the supplemental bits. With S bits/sample of the supplemental quantizer transmitted to the decoder, the rate is $D = M + S$ bits/sample, and the quantizing distortion is very close to that of a conventional codec with D bits/sample.

Errors in the two bit streams have different effects on the decoder output. Errors in the M, minimal bits, are enhanced by the decoder integrator, which has no effect on errors in the S, supplemental bits. This situation compares favorably with conventional DPCM, where all errors are integrated at the decoder. It also has implications for forward error correction in embedded DPCM. Figures 1 and 2 will be further explained in Section II.

1.2 The scope of this paper

Our principal contribution in this paper is an analysis of the combined effects of granular quantizing distortion and transmission errors on the mean-square error of embedded DPCM. The analysis is quite general: special cases include Pulse Code Modulation (PCM) ($M = 0$) and conventional DPCM ($S = 0$). The formulas for the noisy-

* Based on the structure of Fig. 2, Jayant has recently described an enhanced supplemental quantizer (called an explicit noise coder) that uses memory and delay to improve speech quality.[9]

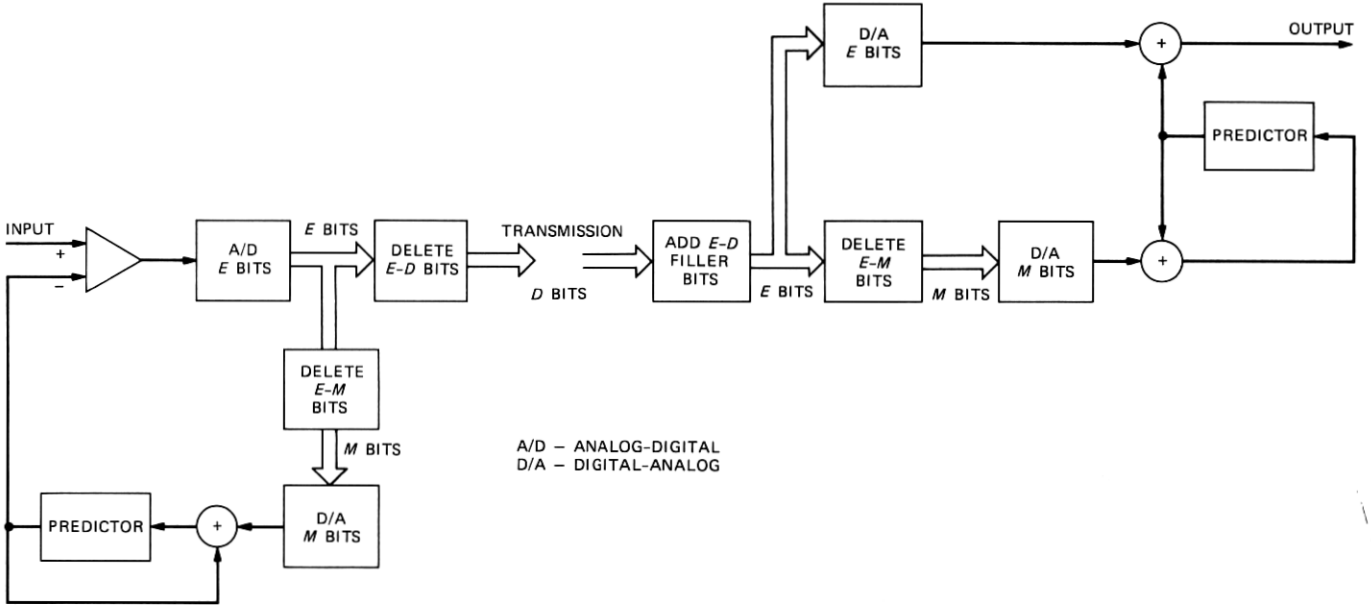

Fig. 1—Embedded DPCM encoder and decoder. Because both predictors operate on the same signal (with resolution M bits/sample) performance is unaffected by errors due to bit-rate adjustment. The channel can transmit between M bits/sample and E bits/sample.

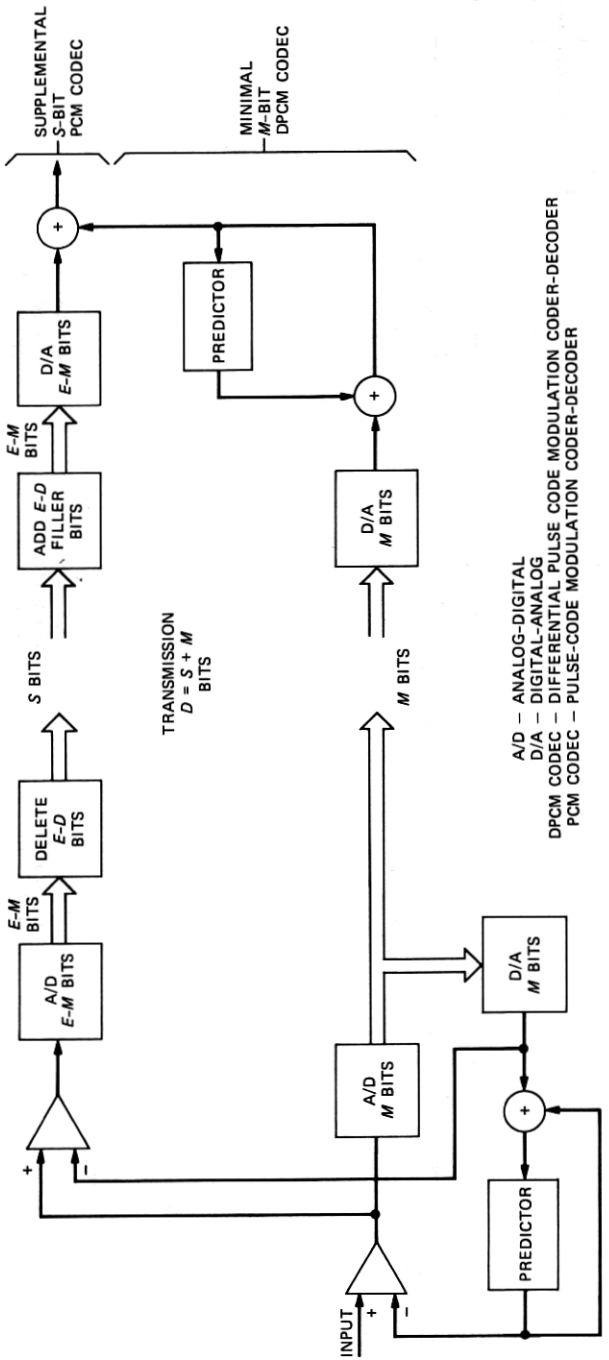

Fig. 2—Embedded DPCM encoder and decoder. E-bit analog-to-digital conversion is shown as a two-stage, successive-approximation process. All M minimal bits are transmitted. S, the number of supplemental bits transmitted, can range from 0 to E–M.

channel performance of conventional DPCM are new, and the specialization to PCM is more precise than previous work on the subject,[10-12] which includes several approximations that are accurate for multibit ($\geq$ 6-bit) quantizers, but are rather imprecise at lower bit rates. The method of analysis has the advantage of separating source effects from transmission effects. The source effects include the characteristics of the analog input signal and the codec design parameters. The transmission effects include modulation and demodulation, the channel, forward error correction, and diversity reception.

The main result is eq. (61), in which the transmission effects are contained in the discrete probability function $P(l)$, where l is an index of binary error patterns. The other symbols in (61) are source parameters and functions of source parameters. After deriving (61) we apply it to specific transmission environments and present, in Table VI, specialized formulas that are convenient for numerical computation.

In all, there are 78 formulas in Sections III through VI, most of them intermediate steps in derivations of a few key results. Anticipating that few readers will require all these details we provide here a summary of the analysis and we display a few numerical results. Sections I, II, and VII contain the main ideas of our work and sufficient information to allow readers to perform, on hand calculators, computations similar to the ones we present.

Section III introduces the notations for the signals and errors in the M-bit minimal DPCM codec and the S-bit supplementary PCM codec of Fig. 2. The analysis of Section III leads to (2), which expresses the sampled-data error sequence as a function of quantization errors, transmission errors, and integrator characteristics. Section IV begins the analysis of the mean-square value of (2) by deriving (35), the ratio of the mean-square codec input to the mean-square value of the encoder difference signal. Section V defines A factors, which are conditional mean squares of the errors due to specific binary error patterns, and derives (61), the general signal-to-noise ratio (s/n) formula. Section VI adapts (61) to specific transmission models and provides guides to numerical computation.

1.3 Examples of numerical results

Figure 3 shows the performance of embedded DPCM in four transmission environments, all of them employing Coherent Phase Shift Keying (CPSK) modulation at 32 kb/s in a white-Gaussian-noise channel. The encoder operates at 32 kb/s (8-kHz sampling, 4 bits/sample), and in format 1 all of this information is transmitted. Figure 3 indicates that when the channel s/n falls below 10 dB, the audio s/n deteriorates rapidly. In format 2, the least significant bit of each DPCM code word is deleted, and the remaining 3 bits/sample are

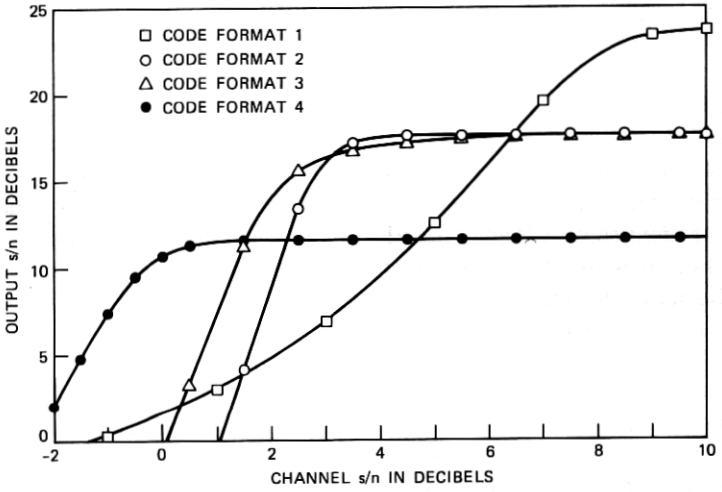

Fig. 3—Performance of embedded DPCM in four transmission environments.

protected by a rate 3/4 convolutional code. Although there is more quantizing noise than in format 1 (the s/n is 6 dB lower in the absence of transmission errors), the convolutional code permits accurate reception of the transmitted bit stream at channel s/n's down to 3 dB. Going one step further with this approach to channel coding, we have format 4, in which 16 kb/s of speech data are transmitted under the protection of a rate 1/2 code. The threshold of essentially error-free performance is now extended down to a channel s/n of about 0 dB.

In code format 3 the speech transmission rate is 24 kb/s, as in format 2, but now only 2 of the 3 bits/sample are protected by the convolutional code, which has rate 2/3. The threshold of curve 3 in Fig. 3 is about 1 dB lower than that of curve 2. On the other hand, format 3 is slightly worse than format 2 in intermediate channel conditions (s/n's between 3 and 5 dB). Over this range, format 2 is essentially error free, while format 3 is affected by errors in the unprotected third bit of each code word. The effect is small, however, because these errors are not amplified at the decoder.

With conventional, rather than embedded, DPCM, the corresponding picture, Fig. 4, is rather different, especially with respect to format 3. Here channel errors in the unprotected third bit are amplified by the integrator at the decoder. The result is a noticeably lower output s/n relative to format 2 (all three bits protected) when the channel s/n is between 3 and 6 dB. On the other hand, in clear channels the greater accuracy of prediction in the conventional encoder causes the output s/n of conventional DPCM at 24 kb/s (formats 2 and 3) and

32 kb/s (format 1) to be about 0.7 dB higher than that of embedded DPCM.

Figure 5, which applies to 24 kb/s speech transmission with a rate 2/3 code, summarizes the performance differences between conventional and embedded DPCM. Conventional DPCM has somewhat lower quantizing noise, which is reflected in the higher s/n in good channels. In intermediate conditions, when errors in the unprotected

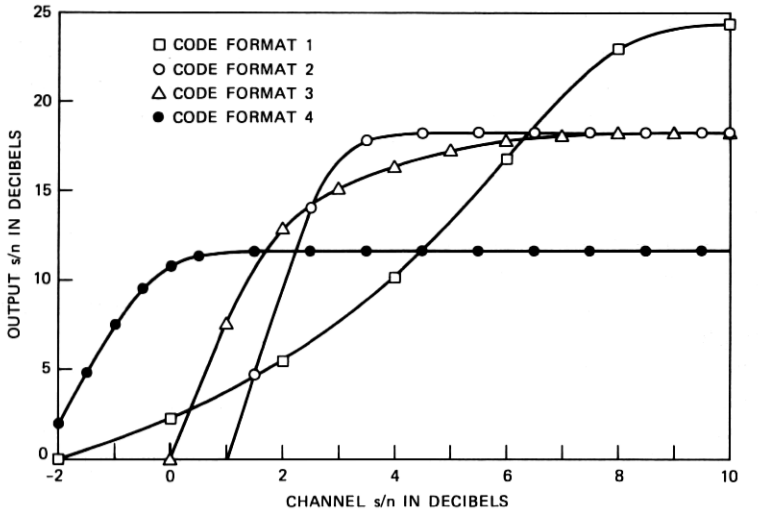

Fig. 4—Performance of conventional DPCM in four transmission environments.

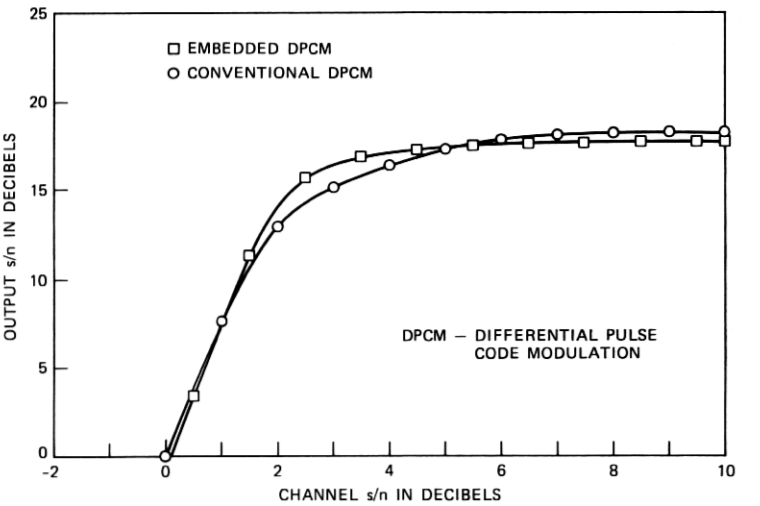

Fig. 5—A 24-kb/s speech transmission with a rate of 2/3 code (Format 3) used to summarize performance differences between embedded and conventional DPCM.

bit influence performance, embedded DPCM is better because the effects of these errors are not amplified at the decoder. In very difficult channels, errors in the two coded bits dominate performance and the s/n's of conventional and embedded DPCM are virtually equal.

II. EMBEDDED DPCM SIGNAL PROCESSING

Figure 1 shows the signal processing operations that take place in embedded DPCM encoding, transmission, and decoding. While the analog-to-digital converter at the encoder generates E bits/sample, the resolution of the signal presented to the integrator is limited to M bits/sample, where M is the minimum bit rate of the transmission system. The transmitted bit rate, D, can vary between M and E. At the receiver E–D filler bits are appended to the incoming signal. As in the encoder, E–M bits are deleted at the integrator input so that in the absence of transmission errors the encoder integrator and the decoder integrator produce the same approximation signal. When this signal is added to the full-resolution (D bits) quantizing error, the sum has nearly the quality of a conventional DPCM signal with D bits/sample.

While Fig. 1 demonstrates practical implementations, Fig. 2, which is equivalent, is easier to analyze. It represents the analog-to-digital conversion as a two-step, successive-approximation process. First the input to the converter is represented by M bits/sample. Then the error of this representation is processed by another analog-to-digital converter with E–M bits/sample. Taken together, the two digital signals comprise an E bits/sample representation of the DPCM difference signal. All of the M bits of the minimal analog-to-digital converter are transmitted. The other E–M bits are subject to deletion by the transmission system. At the receiver the minimal, M-bit signal is processed by a conventional DPCM decoder. The result is added to the supplemental, $S = D - M$ bit representation of the DPCM error signal to produce the system output.

III. SIGNAL ANALYSIS

3.1 Error sequence

To analyze Fig. 2, we introduce Fig. 6, which shows the signals that appear in the analysis and defines their notations. We are interested in the overall error signal

$$e(k) = x'(k) - x(k), \tag{1}$$

the difference between decoder output and encoder input. In particular we will derive the formula

$$e(k) = n_D(k) + e_D(k) + \sum_{i=1}^{\infty} b_i e_M(k - i), \tag{2}$$

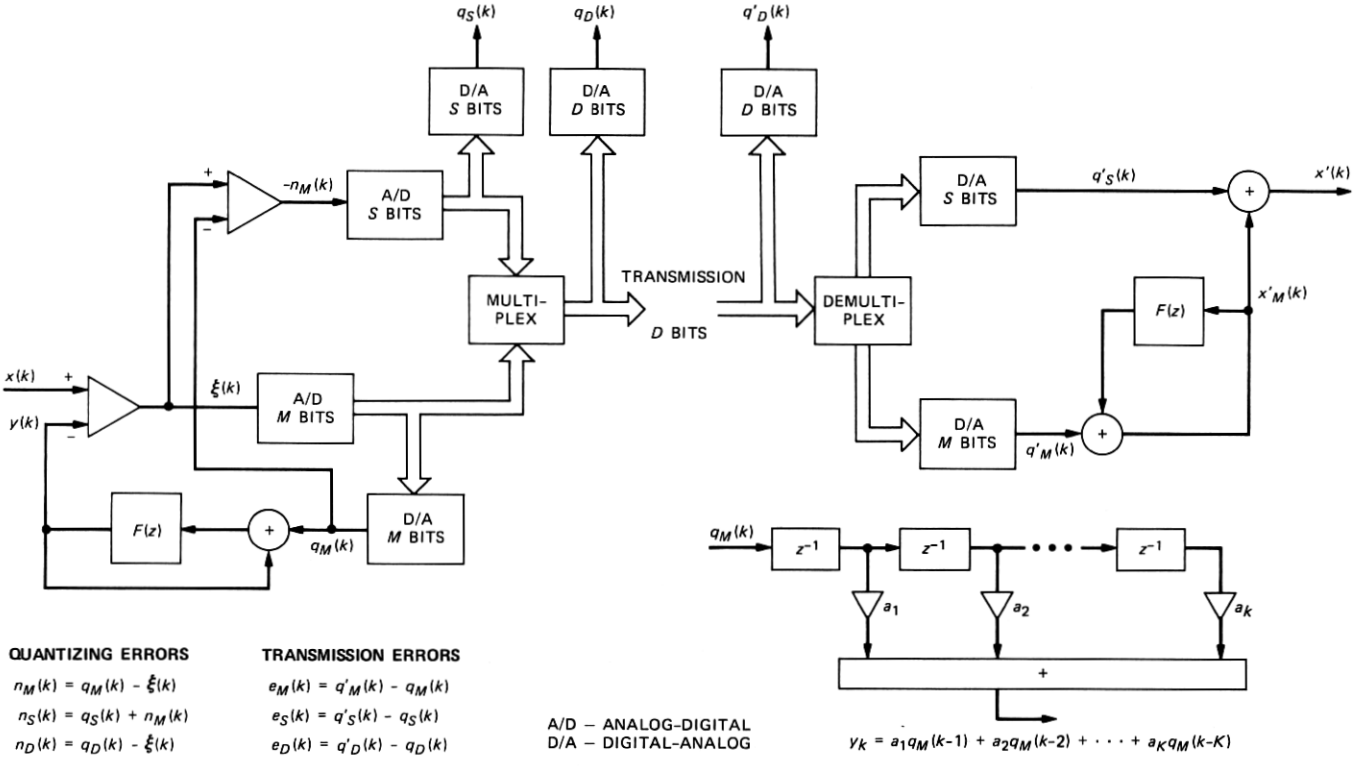

Fig. 6—The signal-processing operations of Fig. 2 and the notation used to analyze them. Three new digital-to-analog converters define signals that appear in the analysis.

where $n_D(k)$ is the quantization noise of the two-stage, D-bit analog-to-digital conversion, $e_D(k)$ is the effect of a transmission error on the entire D-bit transmitted code word, and $e_M(k)$ is the effect of a transmission error on the minimal, M-bit DPCM code word. The coefficients b_i are related to the predictor coefficients $a_1, a_2, \cdots a_K$ according to (12).

Formally,

$$e_M(k) = q'_M(k) - q_M(k), \tag{3}$$

the difference between the quantized inputs to the decoder and encoder integrators. To define $n_D(k)$ and $e_D(k)$, we view the combined code word with $M + S = D$ bits as a digital representation of $\xi(k) = x(k) - y(k)$. A D-bit digital-to-analog converter would produce the quantized signal $q_D(k)$, and so we have the definition of quantization error:

$$n_D(k) = q_D(k) - \xi(k). \tag{4}$$

At the receiver, where the D bits/sample are possibly corrupted by transmission errors, a digital-to-analog converter would produce $q'_D(k)$. The transmision error is

$$e_D(k) = q'_D(k) - q_D(k). \tag{5}$$

In the remainder of Section III we derive eq. (2); in Section IV and V we analyze its mean square.

3.2 Derivation of the error sequence

Here the signal analysis is facilitated by the transform notation of Table I. The reader may verify that the output of the minimal encoder, $Q_M(z)$, is related to input and quantizing noise[8] by

$$Q_M(z) = [X(z) + N_M(z)][1 - F(z)]. \tag{6}$$

Table I—Transform notation for codec signals

Encoder Signal	Description	Decoder Signal
$X(z)$	Encoder input, decoder output	$X'(z)$
	Minimal decoder output	$X'_M(z)$
$Y(z)$	Approximation signal	$Y'(z)$
$Q_M(z)$	M-bit representation of $X(z) - Y(z)$	$Q'_M(z)$
$N_M(z)$	$Q_M(z) - [X(z) - Y(z)]$ Quantizing error in $Q_M(z)$ $Q'_M(z) - Q_M(z)$ Transmission error in $Q'_M(z)$	$E_M(z)$
$Q_S(z)$	S-bit representation of $-N_M(z)$	$Q'_S(z)$
$N_D(z)$	$Q_S(z) + N_M(z)$ Quantizing error in $Q_S(z)$ $Q'_S(z) - Q_S(z)$ Transmission error in $Q'_S(z)$	$E_S(z)$
$F(z)$	Predictor $\sum_{i=1}^{K} a_i z^{-1}$	$F(z)$

In the minimal decoder

$$X'_M(z) = \frac{Q'_M(z)}{1 - F(z)}, \tag{7}$$

which leads to

$$X'_M(z) = X(z) + N_M(z) + \frac{E_M(z)}{1 - F(z)}. \tag{8}$$

In the supplemental encoder,

$$Q_S(z) = -N_M(z) + N_D(z), \tag{9}$$

and at the decoder

$$Q'_S(z) = -N_M(z) + N_D(z) + E_S(z). \tag{10}$$

Combining (8) and (10) we have the output of the entire decoder,

$$X'(z) = X'_M(z) + Q'_S(z) = X(z) + N_D(z) + E_S(z) + \frac{E_M(z)}{1 - F(z)}. \tag{11}$$

To transform (11) to time-domain notation, we defined b_i, $i = 0, 1, 2, \cdots$, to be the inverse z transform of $1/(1 - F)$, such that

$$\frac{1}{1 - F(z)} = \sum_{i=0}^{\infty} b_i z^{-i}. \tag{12}$$

Then we have

$$x'(k) = x(k) + n_D(k) + e_S(k) + \sum_{i=0}^{\infty} b_i e_M(k - i), \tag{13}$$

and the error is

$$\begin{aligned} e(k) &= x'(k) - x(k) \\ &= n_D(k) + e_S(k) + e_M(k) + \sum_{i=1}^{\infty} b_i e_M(k - i), \end{aligned} \tag{14}$$

where we have substituted $b_0 = 1$. Equation (14) is identical to (2) because

$$e_D(k) = e_M(k) + e_S(k). \tag{15}$$

IV. MEAN-SQUARE ERROR

The square of (2) is

$$\begin{aligned} e^2(k) = [n_D(k) + e_D(k)]^2 &+ \sum_{i=1}^{\infty} b_i^2 e_M^2(k - i) \\ &+ 2 \sum_{i=1}^{\infty} b_i [n_D(k) + e_D(k)] e_M(k - i) \\ &+ 2 \sum_{i=1}^{\infty} \sum_{j=i+1}^{\infty} b_i b_j e_M(k - i) e_M(k - j). \end{aligned} \tag{16}$$

To analyze the mean value of (16), we assume that the sequence $\{x(k)\}$ is drawn from a stationary ergodic random process. In our derivations we ignore all correlations in (16) between nonsimultaneous samples. That is, we assume

$$E\{[n_D(k) + e_D(k)]e_M(k - i)\} \approx 0; \qquad i \geq 1 \tag{17}$$

and

$$E\{e_M(k - i)e_M(k - j)\} \approx 0; \qquad i \neq j. \tag{18}$$

Equation (17) indicates that the overall error (quantizing plus channel distortion) in the kth sample is uncorrelated with errors in other samples of the minimal M-bit quantized samples. Equation (18) states that errors in different minimal samples are uncorrelated. These approximations are accurate because the sequence of samples at the input to a DPCM quantizer is decorrelated by the differential coding process and because transmission errors affecting different code words are independent or only weakly correlated.

The approximations, (17) and (18), remove the last two sums from the expected value of (16), leaving

$$E\{e^2(k)\} = E\{[n_D(k) + e_D(k)]^2\} + b_P E\{e_M^2(k)\}, \tag{19}$$

in which we summarize the influence of the predictor in

$$b_P = \sum_{i=1}^{\infty} b_i^2. \tag{20}$$

The expectations in (19) are related to the quantization and transmission of $\xi(k)$, the DPCM difference signal. In Section V, we present a complete theory of the errors due to these operations. While this theory relates these errors to $\sigma_\xi^2 = E\{\xi^2(k)\}$, we are ultimately interested in the s/n of the codec input, $x(k)$:

$$s/n = E\{x^2(k)\}/E\{e^2(k)\} = \sigma_x^2/\sigma_e^2. \tag{21}$$

To find this quantity, we will now derive σ_x^2/σ_ξ^2 and then combine it with the results of Section V. To begin the derivation, we refer to Fig. 6 and verify

$$Y(z) = F(z)[X(z) + N_M(z)], \tag{22}$$

which leads to

$$\xi(k) = x(k) - y(k) = x(k) - \sum_{i=1}^{K} a_i x(k - i) - \sum_{i=1}^{K} a_i n_M(k - i). \tag{23}$$

We write the mean-square value of (23) as

$$\sigma_\xi^2 = E\left\{\left[x(k) - \sum_{i=1}^{K} a_i x(k - i)\right]^2\right\} + E\left[\sum_{i=1}^{K} a_i n_M(k - i)\right]^2$$
$$- 2E\left\{\left[x(k) - \sum_{i=1}^{K} a_i x(k - i)\right]\left[\sum_{i=1}^{K} a_i n_M(k - i)\right]\right\}. \tag{24}$$

The first term in (24) depends on the spectral properties of $x(k)$ and on the predictor. The ratio of σ_x^2 to this quantity is called the prediction gain,

$$G = \sigma_x^2 / E\left\{\left[x(k) - \sum_{i=1}^{K} a_i x(k-i)\right]^2\right\}. \tag{25}$$

It indicates that extent to which the predictor (in the absence of quantization) reduces the mean-square value of the signal to be quantized. Formally we have

$$G^{-1} = \sum_{j=0}^{K} \sum_{i=0}^{K} a_i' a_j' r_{i-j}, \tag{26}$$

in which $a_0' = 1$, $a_i' = -a_i$, $i = 1, 2, \cdots, K$, and r_n is a normalized covariance coefficient of the stationary input,

$$r_n = E\{x(k)x(k+n)\}/\sigma_x^2. \tag{27}$$

In evaluating the second and third terms of (24), we ignore correlation between different quantizing-noise samples and correlations between quantizing-noise samples and samples of the codec input. Thus we use (18) and the approximation

$$E\{n_M(k)x(j)\} \approx 0. \tag{28}$$

This allows us to write

$$\sigma_\xi^2 = G^{-1}\sigma_x^2 + a_P E\{n_M^2(k)\}, \tag{29}$$

where we define

$$a_P = \sum_{i=1}^{K} a_i^2. \tag{30}$$

The noise component of (29), which depends on the quantizer overload point and on the statistical properties of $\xi(k)$, is analyzed in Section V, where we restrict our attention to granular quantizing noise and derive $\sigma_q^2(B)$, the noise power of a B-bit quantizer with unity overload point. If the actual overload point is ξ_{max}, the noise power of the M-bit minimal quantizer is

$$E\{n_M^2(k)\} = \xi_{max}^2 \sigma_q^2(M) \approx \Delta_M^2/12. \tag{31}$$

The quantizer step size is

$$\Delta_M = \xi_{max} 2^{-(M-1)}, \tag{32}$$

and the approximation would be exact if $n_M(k)$ were uniformly distributed over the range $-\Delta_M/2$ to $\Delta_M/2$. Table II presents $\sigma_q^2(B)$ numerically and indicates the fractional error due to the above approximation. A parameter in Table II is the dimensionless load factor

Table II—Quantizing noise

Load Factor		Gaussian		Exponential	
		2 bits	3 bits	2 bits	3 bits
1.78	Noise power $\sigma_q^2(B)$	0.02066	0.005198	0.02189	0.005276
	Approximation error*	−0.01	0.00	0.05	0.01
3.16	Noise power $\sigma_q^2(B)$	0.02082	0.005207	0.02394	0.005419
	Approximation error*	0.00	0.00	0.13	0.04
5.62	Noise power $\sigma_q^2(B)$	0.02292	0.005209	0.02885	0.005836
	Approximation error*	0.09	0.00	0.28	0.11

* Relative error of the approximation $\sigma_q^2(B) \approx 2^{-2B}/3$.

$$L = \xi_{\max}/\sigma_\xi. \tag{33}$$

Combining (29), (31), and (33), we arrive at

$$\sigma_\xi^2 = G^{-1}\sigma_x^2 + a_P L^2 \sigma_q^2(M)\sigma_\xi^2, \tag{34}$$

or the quantity we set out to derive:

$$\sigma_x^2/\sigma_\xi^2 = G[1 - a_P L^2 \sigma_q^2(M)]. \tag{35}$$

V. QUANTIZATION NOISE AND TRANSMISSION NOISE IN PCM

5.1 Granular and overload conditions

To analyze (19), we study, statistically, the quantization and transmission of the DPCM difference signal $\xi(k)$. In this type of study it is customary to separate the quantizing error into two components: overload distortion and granular noise. In speech communication this distinction is valuable for predicting subjective quality.[13,14] Moreover, in analyzing DPCM the distinction is essential because, except for a codec with an ideal integrator,[15] ($F(z) = z^{-1}$, which is pathologically vulnerable to transmission errors), there is no theory for computing the mean-square slope-overload distortion. Thus our analysis separates the transmission of clipped samples of $\xi(k)$ from samples subject to granular distortion. Our theory pertains only to the transmission of unclipped samples. For those samples we add two different distortions, quantizing noise and noise due to transmission errors. Unlike slope overload, both of these impairments are essentially uncorrelated with the signal. This gives us confidence that the mean-square sum is a reasonable quality measure.

Formally, we rewrite (19) as

$$\sigma_e^2 = p_{ov}E\{e^2(k) \mid |\xi(k)| > \xi_{\max}\} + p_{gr}E\{e^2(k) \mid |\xi(k)| \leq \xi_{\max}\}, \tag{36}$$

where $\xi(k)$ is the quantizer input and $\xi_{\max}$ is the overload point of the uniform DPCM quantizer. The probability of overload is p_{ov} and $p_{gr} = 1 - p_{ov}$ is the probability of granular quantization. By definition, the

quantizer is overloaded at time k if the quantization error exceeds half of a quantization step, i.e., if

$$|q_D(k) - \xi(k)| > \Delta_D/2. \tag{37}$$

The step size of the D-bit uniform quantizer is

$$\Delta_D = \xi_{\max} 2^{-(D-1)} = \Delta_M/2^{D-M}. \tag{38}$$

Our remaining analysis will be confined to the second expectation on the right side of (36) and in particular to the ratio,

$$s/n = \sigma_x^2/E\{e^2(k) \,|\, |\xi(k)| \leqslant \xi_{\max}\}. \tag{39}$$

To be concise in the remainder of this paper, we will omit the granular condition, $|\xi(k)| \leqslant \xi_{\max}$, from our notation of expected values.

5.2 *Transmission model, normalized quantizer*

To facilitate numerical evaluation of s/n's, we will present three tables of normalized error terms. The normalization relates these errors to a quantizer with a unity overload point and an input with probability density function $p_u(\cdot)$. If the quantizer of interest has an overload point of $\xi_{\max}$ and the input has the probability density $p_\xi(\cdot)$, the relevant errors are table entries scaled by $\xi_{\max}^2$. The two probability densities are related by

$$p_u(u) = \xi_{\max} p_\xi(\xi_{\max} u). \tag{40}$$

To confine our attention to the granular quantization condition, we perform our averages with respect to the conditional probability density

$$p_{gr}(u) = \frac{p_u(u)}{\int_{-1}^{1} p_u(u)du}, \qquad |u| \leqslant 1$$

$$= 0 \qquad |u| > 1. \tag{41}$$

The model is illustrated in Fig. 7. The signal $u = \xi/\xi_{\max}$ is processed by a B-bit analog-to-digital converter with overload point 1 and step size

$$\Delta_B = 2^{-(B-1)}. \tag{42}$$

The digital output of the a/d is i, and the corresponding quantized signal is u_i, which is related to u by the graph in Fig. 7 and by

$u_i = -1 + (i + 0.5)\Delta_B$ when

$$-1 + i\Delta_B \leqslant u < -1 + (i + 1)\Delta_B, \qquad i = 0, 1, \cdots, 2^B - 1. \tag{43}$$

In Fig. 7, the B-bit code word i is transmitted, and i' is received,

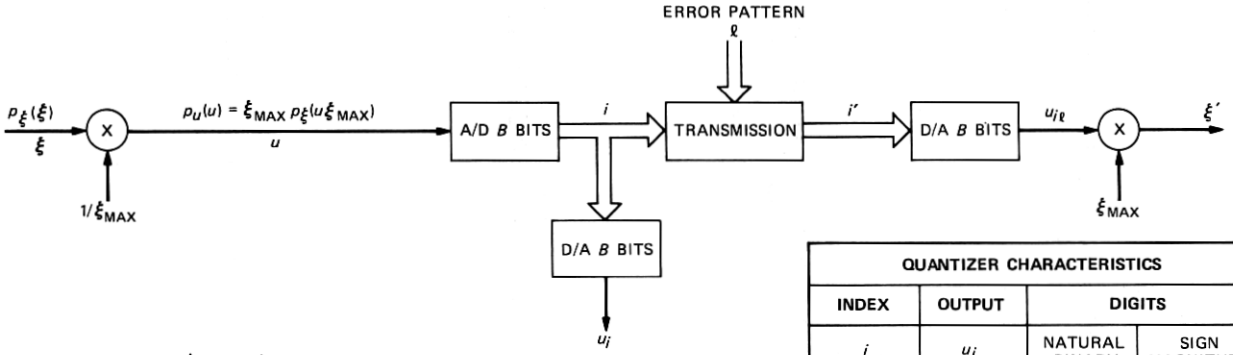

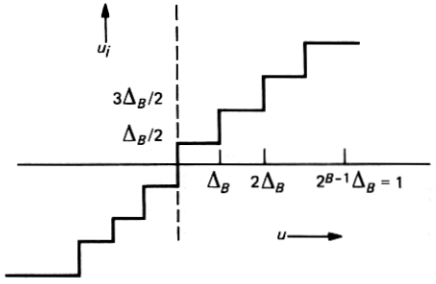

$$A_\ell(B) = E\{(u_{i\ell} - u_i)^2\}$$

$$\tilde{A}_\ell(B) = E\{(u_{i\ell} - u)^2\} - E\{(u_i - u)^2\}$$

A/D – ANALOG-DIGITAL
D/A – DIGITAL-ANALOG

QUANTIZER CHARACTERISTICS			
INDEX	OUTPUT	DIGITS	
i	u_i	NATURAL BINARY	SIGN MAGNITUDE
2^B-1	$1-\Delta_B/2$	111	011
⋮	⋮	⋮	⋮
$2^{B-1}+1$	$\Delta_B/2$	100	000
2^{B-1}	$-\Delta_B/2$	011	100
⋮	⋮	⋮	⋮
1	$-1+3\Delta_B/2$	001	110
0	$-1+\Delta_B/2$	000	111

Fig. 7—Model for analyzing quantizing noise and the effects of transmission errors. The graph and table define the quantizer and two binary number representations.

with the transformation of i to i' characterized by a binary-error pattern with index l, l being an integer in the range 0, $2^B - 1$. To relate the error effect to l, we refer to the natural-binary representation of l and specify that a 1 in the bth *least*-significant position of l causes an inversion of the bth *most*-significant* bit in the binary representation of i. Thus $l = 0$ refers to error-free transmission ($i = i'$); $l = 1$ refers to an error only in the most significant bit; $l = 5$ refers to errors in the first and third most significant bits; etc.

With u the quantizer input and l the binary error pattern, we denote the received sample in Fig. 7, u_{il}. It is helpful to separate the complete error $u_{il} - u$ into quantization-noise and transmission-noise components as follows,

$$u_{il} - u = (u_i - u) + (u_{il} - u_i). \tag{44}$$

5.3 Conditional expectations of transmission-error effects

5.3.1 The general approach

Our goal is to evaluate the mean-square of (44) over the joint distribution of input statistics and binary-error patterns. The key to our analysis is the definition of A factors, which are conditional mean-square errors, each related to a specific binary-error pattern, l. By analyzing these conditional errors, we separate the effects of source characteristics from the effects of transmission characteristics. The source effects are embodied in the A factors; the transmission effects are embodied in probabilities of error patterns. These probabilities govern the weighted addition of the A factors to produce the final result.

This approach to analyzing transmission impairments was introduced by Rydbeck and Sundberg,[10-12] who were mainly concerned with quantizers with 6 to 8 bits/sample. This high resolution admitted various approximations that are inaccurate in the 2- to 4-bit quantizers of greatest interest for embedded DPCM transmission. Thus we proceed to a precise calculation of two types of A factors: conditional expectations related to the isolated effects of digital transmission errors and conditional expectations that include correlations between transmission errors and quantizing noise. In high-resolution quantizers this correlation is negligible, and the two types of A factors are essentially equal.

5.3.2 Analysis

To compute the mean-square value of (44), conditioned on error pattern l, we will identify three important quantities: $\sigma_q^2(B)$, the

* This reversal of the bit ordering of l relative to the binary representation of i will facilitate bookkeeping in subsequent computations.

granular-noise power of a B-bit quantizer; $A_l(B)$, the mean-square effect of error pattern l on the quantized signal u_i; and $\tilde{A}_l(B)$, the overall effect of error pattern l on the mean-square error of the analog output u_{il}.

To derive computationally convenient expressions for $\sigma_q^2(B)$, $A_l(B)$, and $\tilde{A}_l(B)$, we defined the integrals

$$p_i = \int_{v_i}^{v_{i+1}} p_{gr}(u)du \tag{45}$$

$$q_i = \int_{v_i}^{v_{i+1}} (u_i - u)p_{gr}(u)du \tag{46}$$

$$\sigma_{gr}^2 = \int_{-1}^{1} u^2 p_{gr}(u)du, \tag{47}$$

in which v_i is the lower boundary and v_{i+1} is the upper boundary of quantizing interval i:

$$v_i = -1 + i2^{-(B-1)}; \qquad i = 0, 1, \cdots, 2^B. \tag{48}$$

The first integral (45) is the probability of using interval i. The second integral (46) is the average quantization error in interval i. If B is large, Δ_B is small, and $q_i \approx 0$ because u_i is in the center of the quantization interval. The third integral (47) is the mean-square signal when the quantizer is in the granular condition.

Now we write the definitions followed by computational formulas for the quantizing noise and the effects of error pattern l:

$$\sigma_q^2(B) = E(u_i - u)^2 = \sigma_{gr}^2 + \sum_{i=0}^{2^B-1} (2q_i u_i - p_i u_i^2) \tag{49}$$

$$A_l(B) = E(u_{il} - u_i)^2 = \sum_{i=0}^{2^B-1} p_i(u_{il} - u_i)^2 \tag{50}$$

$$\tilde{A}_l(B) = E(u_{il} - u)^2 - E(u_i - u)^2 = A_l(B) + 2\sum_{i=0}^{2^B-1} q_i(u_{il} - u_i). \tag{51}$$

$\tilde{A}_l(B)$, the difference between the total noise and the quantizing noise, includes the correlation between quantization effects and transmission-error effects. In multibit quantizers ($B > 4$) this correlation is small, and $\tilde{A}_l(B) \approx A_l(B)$, an assumption inherent in previous work on PCM. Because low-resolution quantizers are of interest in DPCM, we take account of this correlation in our present work.

Finally, we combine (49), (50), and (51) to write the mean-square value of (44)

$$\epsilon_l^2 = E(u_{il} - u)^2 = \sigma_q^2(B) + \tilde{A}_l(B). \tag{52}$$

5.3.3 Computations

Table III displays formulas for p_i, q_i, and σ_{gr}^2 that apply to inputs with Gaussian and exponential probability density functions. Because the input, u, of the normalized quantizer is related to the input, ξ, of the quantizer with overload point ξ_{max} by $u = \xi/\xi_{max}$, we have

$$\sigma_u^2 = \sigma_\xi^2/\xi_{max}^2 = 1/L^2, \tag{53}$$

where L is the dimensionless load factor defined in (33). Because L is a familiar quantizer design quantity, we have written the formulas in Table III as functions of L.

With the formulas in Table III, it is a simple matter to compute $\sigma_q^2(B)$ precisely. However, for $B \geq 4$ the approximation

$$\sigma_q^2(B) \approx \Delta_B^2/12 = 2^{-2B}/3 \tag{54}$$

is very accurate (within 3 percent of the exact value for $L \leq 5.6$). For $B = 2$ and 3, Table II shows the exact values of $\sigma_q^2(B)$ and the approximation errors

$$[\sigma_q^2(B) - \Delta_B^2/12]/\sigma_q^2(B) \tag{55}$$

for $L = 1.78, 3.16, 5.62$ ($L^2 = 10 \pm 5$ dB).

To compute $A_l(B)$, $\tilde{A}_l(B)$, it is necessary to know $u_{il} - u_i$, which depends on the binary number representation of u_i.

5.3.4 Binary number representations

We consider two representations: natural-binary and sign-magnitude, both defined in Fig. 7. Although in general the $A_l(B)$ and $\tilde{A}_l(B)$ depend on p_i and q_i, there are some special cases that are important and illuminating. For example, in the natural-binary code, the single-error A factors are independent of the signal statistics and of the quantizer. An error in the most significant bit causes $u_{il} - u_i = \pm 1$ provided it is the only error in the B-bit code word. Thus $A_1(B) = 1$. Likewise, any isolated error in the second most significant bit causes an output error of $\pm 1/2$, and in general a single binary error in position b causes the mean-square error

$$A_l(B) = (1/4)^{b-1}; \qquad l = 2^{(b-1)}. \tag{56}$$

In the sign-magnitude code, isolated binary errors in positions $b = 2, 3, \cdots, B$ have the same effects as corresponding errors in the natural-binary code. However, an isolated error in the most significant position transforms u_i to $u_{il} = -u_i$. The mean-square effect is

$$A_l(B) = 4E\{u_i^2\} \approx 4\sigma_u^2. \tag{57}$$

The approximation becomes more and more precise as B increases.

Table III—Formulas for computing A factors and quantizing noise B-bit transmission

General

$v_i = -1 + i2^{-(B-1)}; u_i = v_i + 2^{-B}$

	Gaussian	Exponential
Error integral, $Q(x)$	$\int_x^\infty \frac{1}{\sqrt{2\pi}} e^{-u^2/2} du$	
Probability density, $p(u)$	$\frac{1}{\sqrt{2\pi}} \exp\left[-\frac{(uL)^2}{2}\right]$	$\frac{L}{\sqrt{2}} e^{-\lvert u \rvert L\sqrt{2}}$
Conditional (granular) density, $p_{gr}(u)$	$\frac{p(u)}{1-2Q(L)}; \lvert u \rvert \leq 1$ $0 \quad ; \lvert u \rvert > 1$	$\frac{p(u)}{1-e^{-L\sqrt{2}}}; \lvert u \rvert \leq 1$ $0 \quad ; \lvert u \rvert > 1$
Interval probability, p_i	$\frac{Q(Lv_i) - Q(Lv_{i+1})}{1-2Q(L)}$	$\frac{e^{-v_iL\sqrt{2}} - e^{-v_{i+1}L\sqrt{2}}}{2(1-e^{-L\sqrt{2}})}; 2^{B-1} \leq i \leq 2^B - 1$ $p_{2^B-1-i} \quad ; 0 \leq i \leq 2^{B-1} - 1$
Interval mean noise, q_i	$p_iu_i - \frac{e^{-(Lv_i)^2/2} - e^{-(Lv_{i+1})^2/2}}{L\sqrt{2\pi}[1-2Q(L)]}$	$p_iu_i - \frac{e^{-v_iL\sqrt{2}}\left(v_i + \frac{1}{L\sqrt{2}}\right) - e^{-v_{i+1}L\sqrt{2}}\left(v_{i+1} + \frac{1}{L\sqrt{2}}\right)}{2(1-e^{-L\sqrt{2}})}; 2^{B-1} \leq i \leq 2^B - 1$ $-q_{2^B-1-i} \quad ; 0 \leq i \leq 2^{B-1} - 1$
Conditional mean square, σ_{gr}^2	$\frac{1-2Q(L) - L\sqrt{\frac{2}{\pi}} e^{-L^2/2}}{L^2[1-2Q(L)]}$	$\frac{1-e^{-L\sqrt{2}} - e^{-L\sqrt{2}}(L^2 + L\sqrt{2})}{L^2(1-e^{-L\sqrt{2}})}$

5.4 The s/n of the embedded codec

Referring to (52) and Fig. 7, we have the mean-square difference between ξ' and ξ, over all possible error patterns

$$E\{(\xi' - \xi)^2\} = \xi_{\max}^2 E\{\epsilon_l^2\} = \xi_{\max}^2 \left[\sigma_q^2(B) + \sum_{l=1}^{2^B-1} P(l)\tilde{A}_l(B)\right], \quad (58)$$

where $P(l)$ is the probability of error pattern l. The effect of the transmission errors on the quantized version of ξ is $\xi_{\max}^2 \sum_{l=1}^{2^B-1} P(l)A_l(B)$. Returning to (19), we have two expectations: the first is the combined (quantizing and transmission) noise of a D-bit signal; the second expectation is the noise due to transmission errors in the M-bit minimal signal. Thus, we can write (19) as

$$\sigma_e^2 = \xi_{\max}^2 \left[\sigma_q^2(D) + \sum_{l=1}^{2^D-1} P(l)\tilde{A}_l(D) + b_P \sum_{l=1}^{2^M-1} P(l)A_l(M)\right], \quad (59)$$

where $\xi_{\max}^2 = L^2\sigma_\xi^2$ is related to σ_x^2 by

$$\xi_{\max}^2 = \frac{L^2\sigma_x^2}{G[1 - a_P L^2 \sigma_q^2(M)]}. \quad (60)$$

The s/n, which is the principal subject of this paper, is, therefore,

$$s/n = \frac{G[1 - a_P L^2 \sigma_q^2(M)]}{L^2[\sigma_q^2(D) + \sum_{l=1}^{2^D-1} P(l)\tilde{A}_l(D) + b_P \sum_{l=1}^{2^M-1} P(l)A_l(M)]}. \quad (61)$$

With the exception of the two summations in the denominator, all of the quantities in (61) are properties of the input signal and the codec design parameters. These summations,

$$\sigma_{qt}^2 = \sum_{l=1}^{2^D-1} P(l)\tilde{A}_l(D) + b_P \sum_{l=1}^{2^M-1} P(l)A_l(M) \quad (62)$$

comprise the effects of transmission errors on the performance of embedded DPCM. We analyze them in Section VI.

VI. TRANSMISSION EFFECTS, BINARY-ERROR PROBABILITIES

The 2^D probabilities, $P(l)$, of binary-error patterns are properties of the digital transmission system, which includes a modulator, a channel, a demodulator, possibly a codec for forward error correction, and possibly a means for combining different versions (diversity branches) of the received signal. Depending on these components, the $P(l)$ exhibit properties that facilitate evaluation of the sums in (61). In the following subsections we consider three paradigms: (1) random errors with statistically independent transmission of all bits; (2) slow fading

with the bit-error probability constant over each code word, but independent from word to word; and (3) channel coding that makes all error patterns equally likely.

6.1 Random binary errors

Errors in all bits are statistically independent of each other and occur with probability, P. The probability of error pattern l depends only on w, the Hamming weight of l, i.e., the number of ones in the B-bit binary representation of l. Thus,

$$P(l) = P^w(1 - P)^{B-w} = P^w \sum_{j=0}^{B-w} (-1)^j \binom{B-w}{j} P^j. \tag{63}$$

This expansion leads us to express the summations in (61) as polynomials in P. The coefficients of the polynomial involve the sums of all A factors with a fixed weight, w. Let us denote these sums $S_w(B)$ where, for example,

$$\begin{aligned} S_1(B) &= A_1(B) + A_2(B) + A_4(B) + \cdots + A_{2^{B-1}}(B); \\ S_2(B) &= A_3(B) + \cdots + A_{2^{B-1}+2^{B-2}}(B), \end{aligned} \tag{64}$$

and in general,

$$S_w(B) = \sum_{l_w} A_l(B); \qquad \tilde{S}_w(B) = \sum_{l_w} \tilde{A}_l(B), \tag{65}$$

where l_w is the set of all error patterns with Hamming weight, w. Combining (63) and (65), we can write

$$\sum_{l=1}^{2^B-1} P(l)A_l(B) = \sum_{w=1}^{B} \sum_{j=0}^{B-w} P^{j+w}(-1)^j \binom{B-w}{j} S_w(B). \tag{66}$$

The summations in (66) can be manipulated to form

$$\begin{aligned} \sum_{l=1}^{2^B-1} P(l)A_l(B) &= \sum_{w=1}^{B} P^w \sum_{j=1}^{w} \binom{B-j}{w-j} (-1)^{w-j} S_j(B) \\ &= \sum_{w=1}^{B} P^w T_w(B), \end{aligned} \tag{67}$$

where we define

$$\begin{aligned} T_w(B) &= \sum_{j=1}^{w} \binom{B-j}{w-j} (-1)^{w-j} S_j(B); \\ \tilde{T}_w(B) &= \sum_{j=1}^{w} \binom{B-j}{w-j} (-1)^{w-j} \tilde{S}_j(B). \end{aligned} \tag{68}$$

For the natural-binary and sign-magnitude representations we have

discovered and proved that for any input probability distribution, $T_w(B) = \tilde{T}_w(B) = 0$ for $w \geq 3$. Thus the tranmission term in (61) is

$$\sigma_{qt}^2 = \sum_{l=1}^{2^{D}-1} P(l)\tilde{A}_l(D) + b_P \sum_{l=1}^{2^{M}-1} P(l)A_l(M)$$
$$= \sum_{w=1}^{2} P^w[\tilde{T}_w(D) + b_P T_w(M)] \tag{69}$$

This formula is valid for channels with random binary errors, and Table IV presents values of $T_1(B)$, $T_2(B)$, $\tilde{T}_1(B)$, and $\tilde{T}_2(B)$ for three quantizer load factors, B = 2–6 bits and Gaussian and exponential inputs.

Table IV—Error constants for uncoded transmission

B	$T_1(B)$	$T_2(B)$	$\tilde{T}_1(B)$	$\tilde{T}_2(B)$	$T_1(B)$	$T_2(B)$	$\tilde{T}_1(B)$	$\tilde{T}_2(B)$
	Sign Magnitude				Natural Binary			
				Gaussian Inputs, Load Factor 1.78				
2	1.146	−0.146	1.085	−0.137	1.250	−0.354	1.194	−0.354
3	1.186	−0.186	1.170	−0.183	1.313	−0.439	1.298	−0.439
4	1.196	−0.196	1.192	−0.195	1.328	−0.461	1.325	−0.461
5	1.198	−0.198	1.197	−0.198	1.332	−0.466	1.331	−0.466
6	1.199	−0.199	1.198	−0.199	1.333	−0.467	1.333	−0.467
				Gaussian Inputs, Load Factor 3.16				
2	0.725	0.275	0.670	0.219	1.250	−0.775	1.167	−0.775
3	0.726	0.274	0.711	0.262	1.313	−0.899	1.292	−0.899
4	0.726	0.274	0.723	0.271	1.328	−0.930	1.323	−0.930
5	0.726	0.274	0.726	0.273	1.332	−0.938	1.331	−0.938
6	0.727	0.273	0.726	0.273	1.333	−0.940	1.333	−0.940
				Gaussian Inputs, Load Factor 5.62				
2	0.510	0.490	0.506	0.273	1.250	−0.990	1.137	−0.990
3	0.460	0.540	0.467	0.485	1.313	−1.165	1.292	−1.165
4	0.460	0.540	0.461	0.527	1.328	−1.196	1.323	−1.196
5	0.460	0.540	0.460	0.537	1.332	−1.204	1.331	−1.204
6	0.460	0.540	0.460	0.539	1.333	−1.206	1.333	−1.206
				Exponential Inputs, Load Factor 1.78				
2	0.943	0.057	0.898	0.000	1.250	−0.557	1.176	−0.557
3	0.958	0.042	0.950	0.024	1.313	−0.667	1.296	−0.667
4	0.964	0.036	0.962	0.031	1.328	−0.692	1.324	−0.692
5	0.966	0.034	0.965	0.033	1.332	−0.698	1.331	−0.698
6	0.966	0.034	0.966	0.033	1.333	−0.700	1.333	−0.700
				Exponential Inputs, Load Factor 3.16				
2	0.693	0.307	0.660	0.168	1.250	−0.807	1.147	−0.807
3	0.667	0.333	0.670	0.285	1.313	−0.958	1.291	−0.958
4	0.666	0.334	0.668	0.321	1.328	−0.990	1.323	−0.990
5	0.666	0.334	0.667	0.330	1.332	−0.998	1.331	−0.998
6	0.666	0.334	0.667	0.333	1.333	−1.000	1.333	−1.000
				Exponential Inputs, Load Factor 5.62				
2	0.537	0.463	0.527	0.205	1.250	−0.963	1.111	−0.963
3	0.465	0.535	0.492	0.430	1.313	−1.160	1.287	−1.160
4	0.459	0.541	0.468	0.512	1.328	−1.198	1.323	−1.198
5	0.458	0.542	0.461	0.534	1.332	−1.206	1.331	−1.206
6	0.458	0.542	0.459	0.540	1.333	−1.208	1.333	−1.208

6.2 Slow fading

Now the binary-error probability is a random variable that is constant over each code word but varies from word to word. In this case the effects of digital errors can be calculated as in (69) but with the average values $\overline{P^w}$ replacing P^w. These averages are computed over the distributions of channel s/n's that govern the random fluctuation of P from one code word to the next.

6.3 Error-correcting codes

To analyze the performance of embedded DPCM protected by an error-correcting channel code, we make three simplifying approximations. The first one, which pertains to the error-correcting code, states that when there is a decoding error, all error patterns are equally likely. Thus we assume that if the C most significant DPCM bits are protected by the code,

$$P(l) = \frac{1}{2^C - 1} P_W = \frac{1}{2^{C-1}} P_e, \qquad l = 1, 2, \cdots, 2^C - 1, \tag{70}$$

where P_W is the word-error probability and P_e is the binary-error probability of the channel code. They are related by

$$P_W = \frac{2^C - 1}{2^{C-1}} P_e. \tag{71}$$

The other two approximations apply when $C < D$, so that the C most significant DPCM bits are protected and the other D–C bits are uncoded. To simplify computations for this case, we (1) ignore simultaneous errors in the protected and unprotected parts of the D-bit word and (2) ignore multiple errors in the unprotected part. We consider separately three different relationships among C, the number of coded bits; D, the length of the entire DPCM code word; and M, the number of bits in the minimal quantizer.

6.3.1 Entire code word protected ($M \leq D = C$)

In this case $P(l)$ may be calculated according to (70) for all D-bit error patterns, $l = 1, 2, \cdots, 2^{D-1}$. This value of $P(l)$ is constant throughout the first sum in (62). In the second sum we have the probability of M-bit error patterns. For each M-bit error pattern there are 2^{D-M} D-bit patterns. Hence $P(l)$ in the second sum of (62) is higher by the factor 2^{D-M} than $P(l)$ in the first sum. Because each sum in (61) is a constant probability times a sum of A factors, we write

$$\sigma_{qt}^2 = \frac{1}{2^{C-1}} P_e[\hat{A}_{sum}^{(D)}(D) + b_P 2^{D-M} A_{sum}^{(M)}(M)], \tag{72}$$

where we define the sum of the first $2^C - 1$ A factors

$$\tilde{A}^{(C)}_{\text{sum}}(D) = \sum_{l=1}^{2^C-1} \tilde{A}_l(D); \qquad A^{(C)}_{\text{sum}}(D) = \sum_{l=1}^{2^C-1} A_l(D). \tag{73}$$

Table V contains numerical values of $\tilde{A}_{\text{sum}}$ and A_{sum} for the sets of conditions of interest to us here.

6.3.2 *Entire minimal code word, parts of the supplemental code word protected ($M \leq C < D$)*

In this event we assume that all of the unprotected bits have the binary-error probability P and that as before the protected bits have binary-error probability P_e. Furthermore, we set to 0 the probability of simultaneous errors in the protected and unprotected parts of the code word. (These errors occur with probability related to P_eP.) We also set to 0 the probability of multiple errors in the unprotected part of the code word (which occur with probability less than P^2). Thus we break the first sum in (61) into two parts. The first part accounts for

Table V—Error constraints $A^{(C)}_{\text{sum}}(B)$ and $\tilde{A}^{(C)}_{\text{sum}}(B)$ *for coded transmission*

Load Factor		$B=2$		$B=3$			$B=4$			
		$C=1$	$C=2$	$C=1$	$C=2$	$C=3$	$C=1$	$C=2$	$C=3$	$C=4$
					Gaussian Inputs, Sign Magnitude					
1.78		0.90	2.15	0.87	2.11	4.37	0.87	2.10	4.35	8.78
3.16	A	0.47	1.72	0.41	1.56	3.45	0.40	1.52	3.37	6.91
5.62		0.26	1.51	0.15	1.11	2.92	0.13	1.05	2.77	5.84
1.78		0.84	2.03	0.86	2.08	4.31	0.86	2.09	4.34	8.75
3.16	$\tilde{A}$	0.39	1.56	0.39	1.52	3.37	0.39	1.51	3.35	6.86
5.62		0.15	1.28	0.13	1.07	2.84	0.13	1.04	2.75	5.80
					Gaussian Inputs, Natural Binary					
1.78		1.00	2.15	1.00	2.15	4.37	1.00	2.15	4.37	8.78
3.16	A	1.00	1.72	1.00	1.72	3.45	1.00	1.72	3.45	6.91
5.62		1.00	1.51	1.00	1.51	2.92	1.00	1.51	2.92	5.84
1.78		0.95	2.03	0.99	2.12	4.31	1.00	2.14	4.36	8.75
3.16	$\tilde{A}$	0.89	1.56	0.97	1.68	3.37	0.99	1.71	3.43	6.86
5.62		0.78	1.28	0.95	1.46	2.84	0.99	1.50	2.90	5.80
					Exponential Inputs, Sign Magnitude					
1.78		0.69	1.94	0.65	1.81	3.92	0.64	1.78	3.85	7.86
3.16	A	0.44	1.69	0.35	1.41	3.33	0.34	1.35	3.20	6.66
5.62		0.29	1.54	0.15	1.09	2.93	0.13	0.99	2.69	5.83
1.78		0.62	1.80	0.63	1.77	3.85	0.63	1.77	3.83	7.82
3.16	$\tilde{A}$	0.34	1.49	0.33	1.37	3.25	0.33	1.34	3.18	6.62
5.62		0.15	1.26	0.13	1.03	2.83	0.12	0.97	2.67	5.79
					Exponential Inputs, Natural Binary					
1.78		1.00	1.94	1.00	1.94	3.92	1.00	1.94	3.92	7.86
3.16	A	1.00	1.69	1.00	1.69	3.33	1.00	1.69	3.33	6.66
5.62		1.00	1.54	1.00	1.54	2.93	1.00	1.54	2.93	5.83
1.78		0.90	1.80	0.97	1.91	3.85	0.99	1.93	3.90	7.82
3.16	$\tilde{A}$	0.83	1.49	0.95	1.64	3.25	0.99	1.68	3.31	6.62
5.62		0.73	1.26	0.92	1.46	2.83	0.98	1.52	2.90	5.79

errors in the first C (protected) bits when the other D–C bits are error free, $l = 1, 2, \cdots, 2^C - 1$. The second part accounts for single errors in the remaining D–C bits when the first C bits are error free, $l = 2^C, 2^{C+1}, \cdots, 2^{D-1}$. The result is

$$\sigma_{qt}^2 = \frac{P_e}{2^{C-1}} \tilde{A}_{sum}^{(C)}(D) + P \sum_{i=C}^{D-1} \tilde{A}_{2^i}(D) + b_P 2^{C-M} \frac{P_e}{2^{C-1}} A_{sum}^{(M)}(M). \quad (74)$$

In the second term we use the approximation

$$P \approx P(1 - P)^{D-C+1}(1 - P_W) \quad (75)$$

for the probability of a single error in the unprotected part of the code word. A further approximation $\tilde{A}_{2^i}(D) \approx A_{2^i}(D)$ simplifies computation of the second term of (74) because, for natural-binary and sign-magnitude representations, (56) applies for $b > 1$. This allows us to derive

$$\sum_{i=C}^{D-1} A_{2^i}(D) = 4(4^{-C} - 4^{-D})/3 = A_{un}^{(C)}(D). \quad (76)$$

Thus for $M \leq C < D$ we have the formula

$$\sigma_{qt}^2 = \frac{1}{2^{C-1}} P_e[\tilde{A}_{sum}^{(C)}(D) + b_P 2^{C-M} A_{sum}^{(M)}(M)] + P A_{un}^{(C)}(D). \quad (77)$$

6.3.3 Part of the minimal code word protected ($C < M \leq D$)

Just as we decomposed the first sum in (61) into two parts in the previous case, we similarly decompose the second sum when some of the M minimal bits are unprotected. The result is

$$\sigma_{qt}^2 = \frac{P_e}{2^{C-1}} [\tilde{A}_{sum}^{(C)}(D) + b_P A_{sum}^{(C)}(M)] + P[A_{un}^{(C)}(D) + b_P A_{un}^{(C)}(M)]. \quad (78)$$

VII. NUMERICAL RESULTS

The useful computational formulas (61), (62), (69), (72), (77), and (78) are summarized in Table VI. In this section we apply these formulas to illustrate some of the properties of embedded DPCM and its relationship to conventional DPCM.

7.1 Source characteristics

All of our numerical results pertain to a Gauss-Markov input signal with adjacent-sample correlation $r_1 = 0.85$. The codec uses single integration with coefficient $a_1 = 0.85$ and the load factor, $L = \sqrt{10}$. For this configuration the coding gain is $G = 3.6$. If the embedded codec has a minimal quantizer with $M = 2$ bits, C_{source} in Table VI is 0.31. For conventional DPCM $C_{source} = 0.35$ with 3 bits/sample and

Table VI—Signal-to-noise ratio of embedded DPCM

$$\text{s/n} = \frac{C_{\text{source}}}{\sigma_q^2(D) + \sigma_{qt}^2}; \quad C_{\text{source}} = \frac{G[1 - a_P L^2 \sigma_q^2(M)]}{L^2}$$

(a) Notation

Symbol	Description	General Formula	Formula for Single Integration
G	Coding gain	(26)	$(1 - 2a_1 r_1 + a_1^2)^{-1}$
a_P	Predictor gain	(30)	a_1^2
L	Load factor	(33)	
M	Minimal codec bits		
D	Transmitted bits		
b_P	$1 + b_P$ is integrator gain	(20), (21)	$a_1^2/(1 - a_1^2)$
r_1	Adjacent-sample autocorrelation	(27)	
$\sigma_q^2(B)$	Quantizing noise	(49)	$2^{-2B}/3$ or Table II
σ_{qt}^2	Transmission-error effects	(62)	

(b) Error Formulas*

Transmission Format	Error Effect σ_{qt}^2
No channel code (Table IV)	$\sum_{w=1}^{2} P^w[\tilde{T}_w(D) + b_P T_w(M)]$
C bits coded (Table V)	
$M \leqslant D = C$	$\frac{P_e}{2^{C-1}}[\tilde{A}_{\text{sum}}^{(D)}(D) + b_P 2^{D-M} A_{\text{sum}}^{(M)}(M)]$
$M \leqslant C < D$	$\frac{P_e}{2^{C-1}}(\tilde{A}_{\text{sum}}^{(C)}(D) + b_P 2^{C-M} A_{\text{sum}}^{(M)}(M)] + P A_{\text{un}}^{(C)}(D)$
$C < M \leqslant D$	$\frac{P_e}{2^{C-1}}[\tilde{A}_{\text{sum}}^{(C)}(D) + b_P A_{\text{sum}}^{(C)}(M)] + P[A_{\text{un}}^{(C)}(D) + b_P A_{\text{un}}^{(C)}(M)]$

* P: binary-error rate, uncoded bits; P_e: binary-error rate, coded bits; $A_{\text{un}}^{(C)}(D) = 4(4^{-C} - 4^{-D})/3$.

0.36 with 4 bits/sample. Thus the quantizing-noise penalty of the embedded codec is 0.54 dB when 3 bits are transmitted, and 0.68 dB when 4 bits are transmitted. As indicated in Ref. 8 these penalties increase for higher values of L and a_1. They decrease rapidly as M increases.

7.2 Modulation, channel, error-correcting codes

In our numerical examples the modulation is coherent phase shift keying (CPSK) so that in a white-Gaussian-noise channel the binary error probability is

$$P = Q(\sqrt{2\rho}), \tag{79}$$

where ρ is the channel s/n and

$$Q(x) = \frac{1}{\sqrt{2\pi}} \int_x^\infty e^{-t^2/2} dt. \tag{80}$$

Figures 3 and 4 depict performance with three different convolutional

codes. For all of them, we use the following truncated union bound to calculate binary-error probability:

$$P_e = \frac{1}{m} \sum_{i=d}^{d+4} w_i Q(\sqrt{2i\rho}). \tag{81}$$

where $m = 1, 2, 3$ for the rate 1/2, 2/3, and 3/4 codes, respectively, and the coefficients w_i and the free distance, d, characterize the convolutional coder and decoder. The codes considered here are punctured codes[16] with constraint length 5 (16 states in the decoder memory). Table VII contains their coefficients and free distances. The combination of (79) and (81) with the formulas in Table VI produces the curves in Figs. 3, 4, 5, and 8.

For transmission environments other than CPSK in a white-Gaussian-noise channel, there are formulas for P and P_e to be used in place of (79) and (81). There are many families of modulation schemes, channel conditions, error-correcting codes, and reception techniques that are of practical interest. This paper provides the tools for studying their effects on the performance of embedded and conventional DPCM. This is a subject worthy of further investigation.

7.3 Binary number representation

Without forward-error correction, the noise due to transmission errors is dominated by the effects of single errors in the most significant part of the transmitted code word. With the natural-binary representation, an error in the most significant bit always causes a noise impulse of half the peak-to-peak range of the quantizer (56). With the sign-magnitude representation, an error in the sign bit inverts the polarity of the quantized signal, thereby producing a noise impulse of approximately twice the magnitude of the quantizer input

Table VII—Source and channel code formats, convolutional code properties

	Format 1	Format 2	Format 3	Format 4
Source code				
bits/sample	4	3	3	2
bits/second	32K	24K	24K	16K
bits/sample protected	0	3	2	2
Channel code rate	No code	3/4	2/3	1/2
Free distance, d		4	5	7
Weight w_d		22	25	4
w_{d+1}	Error	0	112	12
w_{d+2}	Properties	1687	357	20
w_{d+3}		0	1858	72
w_{d+4}		66964	8406	225

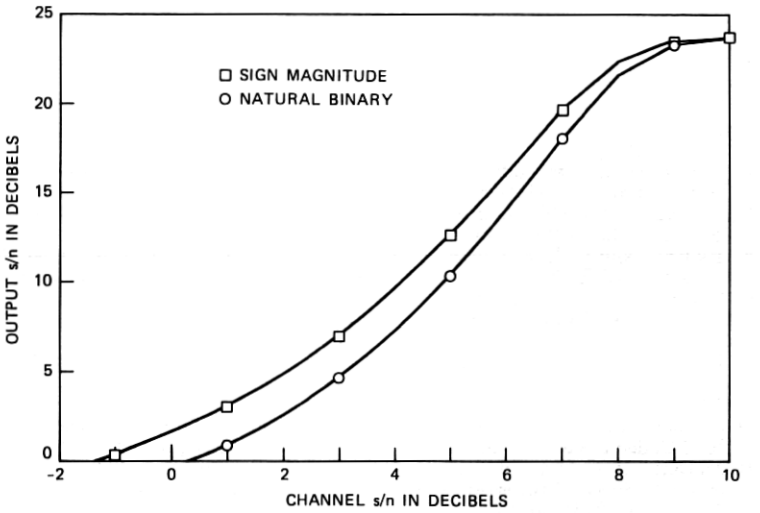

Fig. 8—Performance of embedded DPCM with sign-magnitude and natural-binary representations of quantizer outputs.

(57). Consequently, quantizers employing the sign-magnitude representation are somewhat less affected by transmission errors than quantizers with the natural-binary representation when the input probability distribution has its mode at zero. This is illustrated in Fig. 8, which pertains to uncoded 32 kb/s embedded DPCM transmission. When transmission errors are the dominant distortion, signals represented in the natural-binary format are about 2 dB noisier than signals represented by the sign-magnitude format.

With forward error correction, all error patterns are equally likely, and the two representations have essentially the same s/n.

VIII. ACKNOWLEDGMENT

We thank Lawrence Wong for his helpful comments on this manuscript.

REFERENCES

1. F. S. Boxall, "A Digital Carrier-Concentrator System with Elastic Traffic Capacity," IEEE Trans. Commun., *COM-22*, No. 10 (October 1974), pp. 1636–42.
2. J. A. Sciulli and S. J. Campanella, "A Speech Predictive Encoding Communication System for Multichannel Telephony," IEEE Trans. Commun., *COM-21* (July 1973), pp. 827–35.
3. T. Bially, B. Gold, and S. Seneff, "A Technique for Adaptive Voice Flow Control in Integrated Packet Networks," IEEE Trans. Commun., *COM-28*, No. 3 (March 1980), pp. 325–33.
4. D. J. Goodman and C.-E. Sundberg, "Combined Source and Channel Coding for Variable-Bit-Rate Speech Transmission," B.S.T.J., *62*, No. 7 (September 1983).
5. Proceedings of the 1982 IEEE International Conference on Acoustics Speech and

Signal Processing, Paris, May 1982. Session S8, pp. 954–83, contains four papers on adaptive DPCM at 32 kb/s.
6. J.-M. Raulin, et al., "A 60 Channel PCM-ADPCM Converter," IEEE Trans. Commun., *COM-30,* No. 4 (April 1982), pp. 567–73.
7. D. W. Petr, "32 Kbps ADPCM-DLQ Coding for Network Applications," Record of the IEEE Global Telecommunications Conference, Miami, Florida, November 1982, pp. 239–43.
8. D. J. Goodman, "Embedded DPCM for Variable Bit Rate Transmission," IEEE Trans. Commun., *COM-28,* No. 7 (July 1980), pp. 1040–6.
9. N. S. Jayant, "Variable Rate ADPCM Based on Explicit Noise Coding," B.S.T.J., *62,* No. 3 (March 1983), pp. 657–77.
10. N. Rydbeck and C.-E. Sundberg, "Analysis of Digital Errors in Non-Linear PCM Systems," IEEE Trans. Commun., *COM-24,* No. 1 (January 1976), pp. 59–65.
11. C.-E. Sundberg and N. Rydbeck, "Pulse Code Modulation with Error-Correcting Codes for TDMA Satellite Communication Systems," Ericsson Technics, *32,* No. 1 (1976), pp. 1–56.
12. N. Rydbeck and C.-E. Sundberg, "PCM/TDMA Satellite Communication Systems with Error-Correcting and Error-Detecting Codes," Ericsson Technics, *32,* No. 3 (1976), pp. 195–247.
13. D. J. Goodman, B. J. McDermott, and L. H. Nakatani, "Subjective Evaluation of PCM Coded Speech," B.S.T.J., *55,* No. 8 (October 1976), pp. 1087–109.
14. B. McDermott, C. Scagliola, and D. J. Goodman, "Perceptual and Objective Evaluation of Speech Processed by Adaptive Differential PCM," B.S.T.J., *57,* No. 5 (May–June 1978), pp. 1597–618.
15. L. J. Greenstein, "Slope Overload Noise in Linear Delta Modulators with Gaussian Inputs," B.S.T.J., *52,* No. 3 (March 1973), pp. 387–421.
16. G. C. Clark and J. B. Cain, *Error-Correction Coding for Digital Communications,* New York: Plenum Press, 1981, pp. 237–8, and p. 403.

AUTHORS

David J. Goodman, B.E.E., 1960, Rensselaer Polytechnic Institute; M.E.E., 1962, New York University; Ph.D. (Electrical Engineering), 1967, Imperial College, London; Bell Laboratories, 1967—. Mr. Goodman has studied various aspects of digital communications including analog-to-digital conversion, digital signal processing, subjective assessment of voiceband codecs, and spread spectrum modulation for mobile radio. He is Head, Communications Methods Research Department. In 1974 and 1975 he was a Senior Research Fellow, and in 1983 a Visiting Professor at Imperial College, London, England. Member, IEEE.

Carl-Erik W. Sundberg, M.S.E.E., 1966, and Dr. Techn., 1975, Lund Institute of Technology, University of Lund, Sweden; Bell Laboratories, 1981–1982. Mr. Sundberg is an Associate Professor in the Department of Telecommunication Theory, University of Lund, and a consultant in his field. He is Director of the consulting company SUNCOM, Lund. During 1976 he was with the European Space Research and Technology Centre (ESTEC), Noordwijk, The Netherlands, as an ESA Research Fellow. He has been a Consulting Scientist at LM Ericsson and SAAB-SCANIA, Sweden, and at Bell Laboratories. His research interests include source coding, channel coding (especially decoding techniques), digital modulation methods, fault-tolerant systems, digital mobile radio systems, spread spectrum systems, and digital satellite communication systems. He has published a large number of papers in these areas during the last few years. Senior Member, IEEE; member, SER, Sveriges Elektroingenjörers Riksförening.